Physicochemical Properties and Apatite Precipitation Behavior of Experimental Calcium Silicate-Based Cements Doped with Phosphate Compounds

---

Abstract

Objectives: This study aims to evaluate the solubility, pH, Ca^{2+} release, setting time, and hydroxyapatite (HAp) formation of the tested materials.

Methods: Four study groups were tested: NEX-MTA (NMTA; GC, Japan), NMTA with phosphorylated pullulan (MTA-PPL), NMTA with poly-PS (MTA-polyPS), and Biodentine (BD; Septodont, France). Solubility was measured after 7 and 28 days at 37 °C in deionized water. Ca^{2+} release and pH evaluation were performed after immersion in deionized water at 3 h, 24 h, 7 days, and 28 days using pH and Ca^{2+} meters. Setting times were determined with a Vicat apparatus, and apatite precipitation was evaluated through scanning electron microscopy/energy-dispersive X-ray spectroscopy (SEM/ EDS) and Fourier transform infrared spectroscopy (FTIR) analysis 28 days in phosphate-buffered saline.

Results: NMTA showed the lowest solubility; however, there was no statistically significant difference between NMTA and MTA-polyPS ($P > 0.05$)**.** NMTA exhibited the most alkaline pH at all measured time points. Although MTA-polyPS consistently showed lower pH values than NMTA throughout the observation periods, no statistically significant differences were observed among MTA-polyPS, BD, and MTA-PPL at 28 days ($P > 0.05$). BD released the most Ca^{2+}, with MTA-polyPS releasing the least. BD exhibited the shortest initial and final setting time (9.2 and 42 min, respectively), followed by MTA-polyPS, MTA-PPL, and NMTA. SEM/ EDS and FTIR indicated that MTA-polyPS had the highest apatite precipitation, with Ca/P ratios of 1.70 (NMTA) and 1.79 (MTA-polyPS). MTA-PPL and BD showed no significant apatite precipitation, with Ca/P ratios of 3.93 and 34.9, respectively.

Significance: The incorporation of polyPS into calcium silicate-based cement may enhance apatite precipitation and

accelerate the setting without altering the pH and solubility property.

Keywords: Mineral trioxide aggregate, Calcium silicate cement, Hydroxyapatite, Bioactivity, Endodontics

1. INTRODUCTION

Mineral trioxide aggregate (MTA) is a highly biocompatible calcium silicate-based cement (CSC) that demonstrates positive clinical outcomes in endodontic procedures [1][2]. MTA was the first CSC used in endodontics, and since then, various types of MTA have been developed [3]. MTA is used as pulp capping as an alternative to $Ca(OH)_2$, as it induces dentin development and reduces pulp inflammation [4][5]. Moreover, MTA possesses several advantageous physical properties compared to $Ca(OH)_2$, such as improved sealing, reduced solubility, and greater structural stability [2]. Therefore, MTA has recently been defined as the new gold standard in several endodontic procedures [6]. However, MTA still presents several drawbacks, including challenging handling, extended setting time, poor adhesion to hard dental tissues, and potential for discoloration of the crown [7][8][9]. Improving these CSCs' physiochemical properties and enhancing apatite precipitation bioactivity have driven new-generation CSCs [10][11] .

Indeed, a modern CSC known as Biodentine™ (BD: Septodont, Saint-Maur des Fosses, France) was introduced in 2009 to improve some of the disadvantages aforementioned [12]. BD exhibited a shorter setting time and significantly reduced discoloration compared to conventional MTA, due to the absence of bismuth oxide and the additive of $CaCl_2$ acting as an accelerator and regulated the setting reaction [13][14]. However, BD still presents challenges in handling, does not adhere well to hard dental tissues, and its long-term *in vivo* effectiveness as a pulp-capping treatment remains uncertain [9].

In a recent study, it has been proposed that MTA containing phosphorylated pullulan (PPL) does not present some of the

typical issues of CSCs, particularly the lack of adhesion to hard dental tissues, along with the difficult handling properties [15]. Pullulan (PL) is a polymer derived from the fermentation of black yeast [16]. As a potential biomaterial, pullulan offers several advantages due to its non-toxic nature and the availability of hydroxyl groups within the pyranose rings for substitution with phosphate groups [17][18]. Therefore, phosphorylated pullulan (PPL) has been expected as a carrier for growth factors for bone tissue engineering, where its strong chemical bond that forms between the phosphate groups and hydroxyl group contributes to adhesion with hard tissue [19]. Some studies have already demonstrated that MTA containing PPL (MTA-PPL) exhibits favorable bioactivities, including an excellent healing response in pulp tissue and the ability to induce complete mineral tissue formation when used as a direct pulp capping material [9][20][21].

On the other hand, inorganic polyphosphate (polyP) is composed solely of a chain of phosphate groups connected by high-energy bonds. Perhaps interestingly, this compound is present in every organism and plays roles in a multitude of cellular processes, including phosphate storage, blood coagulation, and pathogenicity [22]. PolyP has been identified in human osteoblasts and is known to have several beneficial effects on bone tissue [23]. It also positively influences apoptosis and the mineralization process [24]. Furthermore, PolyP promotes intracellular calcification, the maturation of bone-related immature cells, and contributes to bone tissue deposition by osteoblasts; it induces alkaline phosphatase (ALP) activity, as well as upregulates the gene expression of osteocalcin and osteopontin [25]. PolyP present enhanced antibacterial properties and dentin-inductive properties, depending on its molecular size (chain length). PolyP is classified into long-chain (polyPL), medium-chain (polyPM), and short-chain (polyPS). It has been advocated that polyPM enhances fibroblast growth factor (FGF) function, accelerates tissue regeneration and bone regeneration, and inhibits bone resorption by osteoclasts, whereas polyPL showed similar activity as polyPM but act as a more efficient inhibitor of bone resorption and inducible nitric oxide,

NO, synthase (iNOS) expression [26]. Moreover, polyPS has been demonstrated to be highly effective in preventing staining of the tooth surface and suppressing its demineralization by binding to the tooth surface [27]. Therefore, polyPS has most potential to strongly adhere to hydroxyapatite (HAp) compared with the other polyP with different chain lengths [28].

This laboratory study aimed to evaluate the solubility, pH, calcium ion release, initial and final setting times, and HAp deposition bioactivity of various MTA cements doped with poly-PS or PPL compared to two commercial cements (MTA and BD). The hypothesis being tested in this study was that the incorporation of polyPS or PPL in an MTA cement would enhance its physicochemical and apatite precipitation behavior.

2. MATERIALS AND METHODS

This laboratory study was approved by the Institutional Ethical Committee of Hokkaido University (2018-9). The present investigation was designed with four experimental groups which are depicted in Table 1.

2.1 Materials

The materials used in this study are also depicted in Table 1. NMTA, an MTA-based CSC was used as a control material, and as the base material to formulate experimental MTA. Hence, several experimental MTA-PPL and MTA-polyPS were generated and used in this study. Biodentine™, a further popular CSC widely applied in various fields of dentistry, was also employed in this study as the control group.

Table 1: Tested and analyzed materials and their composition

Materials	Manufactures	Components
NEX-MTA™ (NMTA)	GC, Tokyo, Japan	Calcium oxide, Bismuth oxide, Silicon dioxide, Aluminum oxide
Mineral trioxide aggregate containing phosphorylated pullulan (MTA-PPL)	GC, Tokyo, Japan	Calcium oxide, Bismuth oxide, Silicon dioxide, Aluminum oxide, Phosphorylated pullulan (5 wt%)
Phosphorylated Pullulan (PPL)	GC, Tokyo, Japan	Pure phosphorylated pullulan
Biodentine™ (BD)	Septodont, Saint Maur des Fosses, France	Powder: Tricalcium silicate, Dicalcium silicate, Calcium carbonate, Zirconium dioxide, Iron oxide Liquid: Calcium chloride, Hydrosoluble polymer
Exclusive Polyphosphate Short chain™ (polyPS)	RegeneTiss, Tokyo, Japan	0.5 mol/L in H_2O

2.2 Specimen Preparation

The following materials were tested in the present investigation:

Group 1 - NMTA: NEX-MTA™, the powder was mixed at a water-to-powder ratio of 1:3 on a glass slab for 1 min according to the manufacturer's instructions.

Group 2 - BD: Biodentine™; the powder was mixed with the liquid according to the manufacturer's instructions: open a Biodentine™ capsule and remove the white cap, use a pipette to dispense five drops of liquid into the capsule, close the capsule with the white cap, and triturate the mixture for 30 s at 4,000 rpm.

Group 3 - MTA-polyPS: Experimental MTA containing Exclusive Polyphosphate Short chain™ (MTA-polyPS); the experimental MTA was prepared by 0.5 mol/L polyPS to NMTA original composition instead of water. The powder was mixed with polyPS solution at a water-to-powder ratio of 1:3 on a glass slab for 1 min in the same technique used in Group 1.

Group 4 - MTA-PPL: the experimental MTA-PPL was prepared by adding to 5 wt% PPL to NMTA. The powder was mixed at a water-to-powder ratio of 1:3 on a glass slab for 1 min in the same technique used in Group 1.

2.3 Solubility

To assess the solubility of the tested materials, silicone molds with an internal diameter of 7.75 mm and a thickness of 1.5 mm were utilized [29]. These were placed on a 1 mm thick glass plate and covered with a cellophane. After being filled with material, the molds were stored at 37 °C and 95 % relative humidity for a duration equal to three times the final setting time. After being removed from the molds, the specimens were weighed on a precision analytical balance with 0.0001 g accuracy (AUX220™; Shimadzu, Japan) - this weight was recorded as the initial (W_0). Subsequently, each specimen was individually placed in a cylindrical polystyrene container holding 7.50 mL of deionized water, ensuring that the material did not encounter the internal surface of the container. The recipients were sealed and stored at 37 °C. After 7 and 28 days, the specimens were taken out of the containers, rinsed with deionized water, and then placed in a desiccator for 24 h. Then, the specimens were weighed on the same balance and this weight was recorded as the final (W_f). The solubility value at 7 and 28 days corresponded to the percentage of weight variation at these times about the W_0, according to the formula:

$$\text{solubility} = (W_f - W_0) \times 100. \quad (1)$$

If any specimen showed signs of disintegration, it was replaced, and the test was repeated. Five specimens were used for each group, and the mean values and standard deviation (%) were calculated to determine the solubility value [30].

2.4 Alkalizing Activity (pH) and Cumulative Calcium Ion Releasing Activity

The specimens for measuring pH and cumulative calcium-releasing activity were prepared and stored in deionized water in the same way as the solubility test. The pH values were recorded using a pH meter (Sension™+PH3; Hach Lange, UK), and Ca^{2+}-releasing activity was measured using a calcium ion meter (pH80+DHS; Dostmann Electronic, Germany) [31] at four times for each experiment: after 3 h, 24 h, 7 and 28 days. All measurements were conducted at 37 °C to simulate physiological conditions. Before measuring, the pH meter was calibrated with solutions of known pH (4.0, 7.0 and 9.0). Before the immersion of the specimens, the pH of the deionized water was checked to avoid any interference. Five measurements were recorded for each group, and the mean values and standard deviation were calculated to obtain the pH value [30][32].

2.5 Initial and Final Setting Time

The setting time was determined using a Vicat apparatus (Contenco, São José da Lapa, MG, Brazil), as recommended by ANSI/ADA 57 [33]. The mixed cements were mixed and placed into silicone molds (10 mm in diameter and 2 mm in height). Five measurements were taken for each group. The Vicat needle was lowered and held in contact with the material's surface for 5 s to assess the setting properties. This procedure was repeated every 60 s, continuing until the indentation test made by the Vicat needle on the material's surface was no longer visible to the naked eye. The test was conducted three times for consistency, and the setting time was established based on the mean value obtained from these repetitions [34]. The initial setting time was measured at 1-min intervals for the first 10 min. The point at which the needle could no longer penetrate to the full depth of 2 mm in the cement was designated as the initial setting time. The final setting time was then measured at 5-min intervals from 10 to 30 min, followed by 1-hour intervals from 30 to 120 min. To accurately pinpoint

the final setting time, measurements were again taken at 1-min intervals as the final setting approached. The specimens were stored in a cabinet maintained at 37 ℃ and 95 % relative humidity during this latest setting steps. The moment when the needle left no visible impression on the specimen was recorded as the final setting time. To confirm that the setting was fully complete, two additional measurements were conducted after the final setting point was determined [35]. Only one trained operator evaluated the setting time throughout the study. The operator was calibrated to determine the endpoint based on the ISO 6876:2012 standard, which defines setting as the time when a standard needle no longer leaves a visible indentation on the sample surface.

2.6 Scanning Electron Microscopy and Energy-Dispersive X-ray Spectroscopy Analysis

The specimens (three specimens per group) were prepared using 10 mm in diameter and 2 mm high in the same manner as those used for solubility test (Section 2.3) and were stored at 37 °C and 95% relative humidity. The ability of the materials to induce apatite precipitation bioactivity was performed by immersing the cement disks at 37 °C in 13 mL phosphate-buffered saline (PBS) for 0 days (baseline) and 28 days. The specimens from each group were mounted on aluminum stubs and coated with gold using a sputter coater (MED 010; Balzers, Balzer, Liechtenstein). They were then examined using an ultra-high-resolution analytical focused ion beam scanning electron microscope (FIB-SEM, Thermo Scientific Scios 2 DualBeam, Waltham, MA, USA) in the secondary electron mode. The FIB-SEM was equipped with an energy-dispersive X-ray spectroscopy (EDS), which operated at 20 kV voltage. During the EDS analysis, each specimen was assessed in six different random spot areas to determine the Ca/P ratio of the crystals formed [36].

2.7 Fourier Transform Infrared Analysis

The specimens (three specimens per group) were prepared as described in Section 2.6 and stored at 37 °C and 95 % relative humidity. These were evaluated via a Fourier-transform infrared (FTIR) micro-spectroscopic system equipped with an attenuated total reflection (ATR) device (Spectrum Two, Perkin Elmer, Madrid, Spain). The specimens were submitted to vibrational chemical analysis in triplicates and the spectra were recorded in the wavenumber range 3000–500 cm^{-1} and with 32 scans at 4 cm^{-1}. The FTIR peaks were analyzed after baseline (0 days) and 28 days in PBS immersion. The data were next processed via subtraction and normalization using the Spectrum 10™ software (Perkin Elmer) to identify the most characteristic inorganic compounds in the specimens.

2.8 Statistical analysis

Statistical analysis was performed using repeated measures ANOVA and two-way ANOVA to assess changes in solubility, pH, Ca^{2+} release, and setting time at each measuring period and between groups. Post hoc comparisons were conducted using Bonferroni and Tukey's HSD tests where appropriate (IBM SPSS Statistics for Windows, Version 28.0, IBM, Armonk, NY, USA). The P-value for statistical significance was set at $\alpha = 0.05$.

3. RESULTS

3.1 Solubility

The results of the solubility test are shown in Fig. 1. NMTA exhibited the lowest solubility at both 7 and 28 days. There were no statistically significant differences in solubility between NMTA and MTA-polyPS at any of the evaluated time

points (P > 0.05). Whereas, MTA-PPL exhibited the highest solubility among all groups at both 7 and 28 days, with statistically significant differences (P < 0.05). The solubility of BD was not significantly different from that of MTA-polyPS (P > 0.05); however, it showed significantly higher solubility than NMTA at 28 days (P < 0.05). There were no significant differences in solubility among NMTA, BD, and MTA-polyPS. Furthermore, no significant differences (P > 0.05) were observed between the 7-day and 28-day groups within each material.

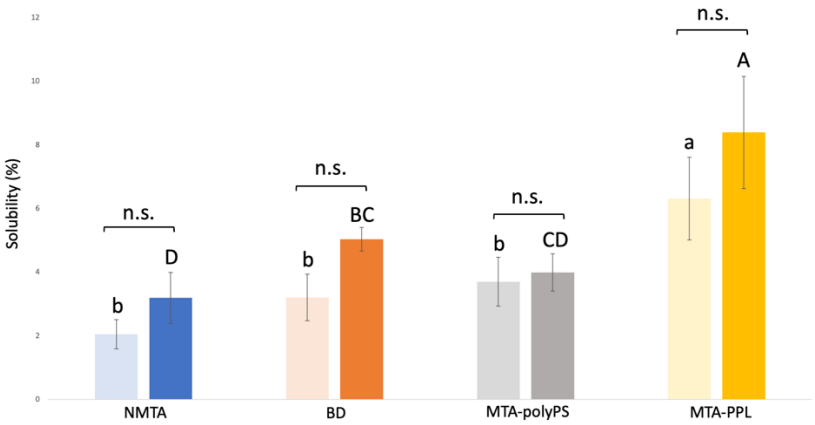

Solubility (%)	NMTA	BD	MTA-polyPS	MTA-PPL
7 days	2.05 ± 0.46	3.21 ± 0.73	3.7 ± 0.77	6.31 ± 1.3
28 days	3.19 ± 0.8	5.04 ± 0.37	3.99 ± 0.59	8.39 ± 1.76

Fig. 1: Average and standard deviation of solubility recorded for each set of specimens. Different lowercase letters indicate statistically significant differences in 7 days solubility. Different capital letters indicate statistically significant differences in 28 days solubility (P < 0.05). There were no significant differences in the solubility between the 7-day and 28-day groups in the same experimental material (P > 0.05).

3.2 Alkalizing Activity (pH) and Cumulative Calcium Ion Releasing Activity

The result of alkalizing activity (pH) is shown in Fig. 2. NMTA exhibited the highest pH in all measurement periods. BD showed the second highest pH values. MTA-PPL exhibited the following highest pH values after BD from 24 hours onward, with no statistically significant differences observed between MTA-PPL and BD at any time point (P > 0.05). In contrast,

MTA-polyPS showed significantly lower pH values than NMTA throughout the observation period ($P < 0.05$), but at 28 days, its pH was not significantly different from that of BD and MTA-PPL. In all experimental materials, the pH values at 7 and 28 days were significantly higher than those at 3 and 24 hours ($P < 0.05$).

The results of cumulative Ca^{2+}-releasing activity are shown in Fig. 3. BD showed the highest cumulative Ca^{2+} release among all groups in all measurement ~~periods~~ points, with statically significant differences ($P < 0.05$). Whereas MTA-polyPS showed the lowest cumulative Ca^{2+} release among all groups at all measurement points, with statically significant differences ($P < 0.05$). The Ca^{2+}-releasing activities of NMTA and MTA-PPL were similar. Statistical analysis showed that there were no differences ($P > 0.05$) between the Ca^{2+}-releasing activity between NMTA and MTA-PPL in 3 h, 24 h, and 7 days. However, the Ca^{2+}-releasing activity of MTA-PPL was significantly higher ($P < 0.05$) than NMTA at 28 days. NMTA and MTA-PPL had significantly higher Ca^{2+}-releasing activities than MTA-polyPS in all observation periods ($P < 0.05$). All groups showed significantly higher Ca^{2+} release at 28 days compared to 3 h and 7 days ($P < 0.05$). In contrast, when comparing Ca^{2+} release between 24 h and 28 days, no significant differences were observed in NMTA and MTA-polyPS ($P > 0.05$), whereas BD and MTA-PPL showed significantly higher values at 28 days ($P < 0.05$).

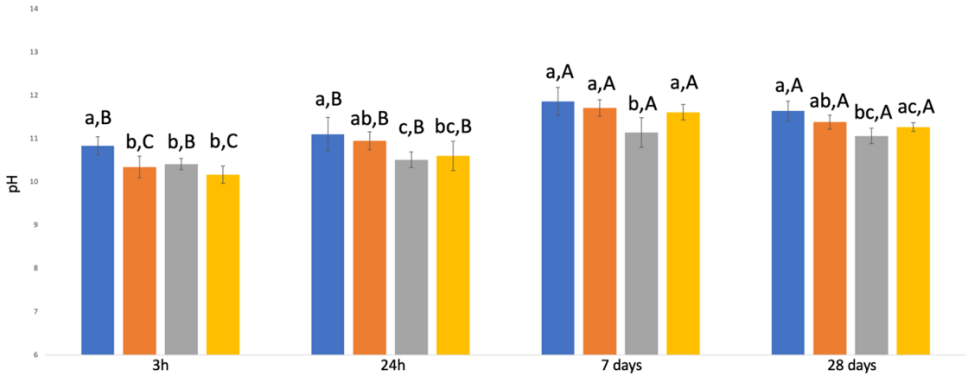

pH	3 h	24 h	7 days	28 days
NMTA	10.83 ± 0.21	11.10 ± 0.39	11.86 ± 0.32	11.64 ± 0.23
BD	10.34 ± 0.25	10.95 ± 0.21	11.71 ± 0.19	11.38 ± 0.16
MTA-polyPS	10.41 ± 0.13	10.51 ± 0.18	11.14 ± 0.34	11.06 ± 0.18
MTA-PPL	10.17 ± 0.20	10.60 ± 0.34	11.61 ± 0.18	11.27 ± 0.10

Fig. 2: Average and standard deviation of pH recorded for each set of specimens. Different lowercase letters indicate statistically significant differences between different experimental materials in the same measuring period ($P < 0.05$). Different capital letters indicate statistically significant differences between the same experimental material in the different measuring periods ($P < 0.05$).

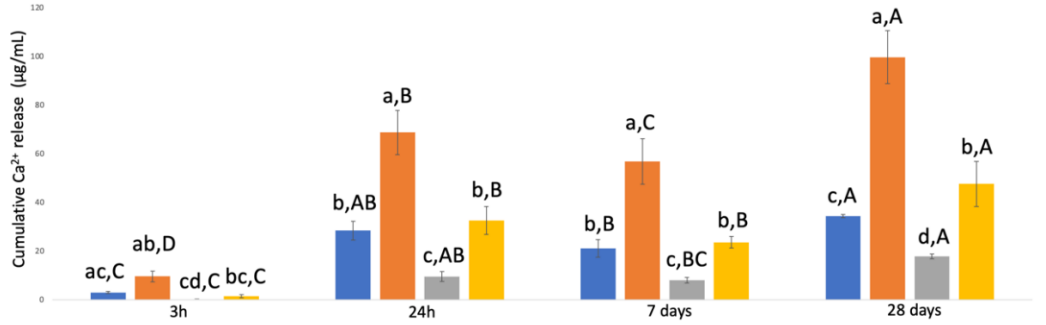

Cumulative Ca^{2+} release (µg/mL)	3 h	24 h	7 days	28 days
NMTA	3.01 ± 0.45	28.48 ± 3.82	21.16 ± 3.54	34.43 ± 0.67
BD	9.63 ± 2.25	68.73 ± 9.06	56.82 ± 9.33	99.62 ± 10.87
MTA-polyPS	0.25 ± 0.10	9.58 ± 2.02	8.07 ± 1.13	17.89 ± 0.99
MTA-PPL	1.45 ± 0.63	32.58 ± 5.76	23.64 ± 2.39	47.63 ± 9.25

Fig. 3: Average and standard deviation of cumulative calcium ion-releasing activity recorded for each set of specimens. Different lowercase letters indicate statistically significant differences between different experimental materials in the same measuring period ($P < 0.05$). Different capital letters indicate statistically significant differences between the same experimental material in the different measuring periods ($P < 0.05$).

3.3 Initial and Final Setting Time

The results of the initial and final setting times are shown below in Fig. 4. Overall, the initial and final setting times of the specimens followed this order: NMTA had the longest setting time, followed by MTA-PPL, MTA-polyPS, and BD with the shortest setting time. NMTA showed the longest setting time compared with the other groups ($P < 0.05$). BD showed the shortest setting times ($P < 0.05$) than all the other tested materials. MTA-polyPS exhibited significantly shorter setting

times compared with NMTA and MTA-PPL ($P < 0.05$). The setting time of MTA-PPL was significantly shorter than NMTA ($P < 0.05$). A statistically significant difference ($P < 0.01$) was observed between the initial and final setting times of each sample.

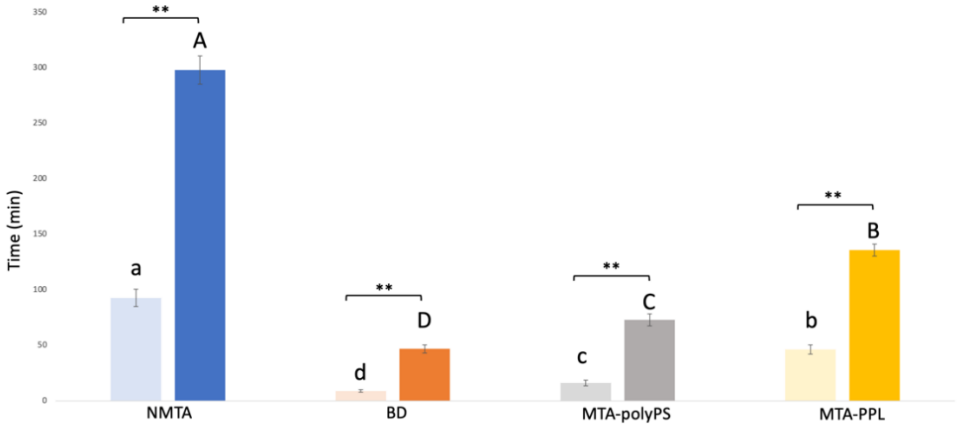

Setting time (min)	NMTA	BD	MTA-polyPS	MTA-PPL
Initial setting time	93 ± 7.8	9.2 ± 1.2	16.4 ± 2.6	46.6 ± 4.2
Final setting time	298.2 ± 12.7	47 ± 3.5	73.2 ± 5.5	136 ± 5.5

Fig. 4: Average and standard deviation of initial and final setting time recorded for each set of specimens. Different lowercase letters indicate statistically significant differences in initial setting time ($P < 0.05$). Different capital letters indicate statistically significant differences in final setting time ($P < 0.05$). The double asterisk on the bar indicates a statistically significant difference ($P < 0.01$) between the initial setting time and the final setting time.

3.4 Scanning Electron Microscopy and Energy-Dispersive X-ray Spectroscopy Analysis

The results of SEM of the surfaces' tested materials (×5000) and SEM/EDS analysis with EDS Ca/P ratio are shown in Fig. 5. Additionally, SEM surface images with the high magnification (×10000) are shown in Fig. 6. In SEM surface images at high magnification, (Fig. 6A) and (Fig. 6C) images exhibited crystal deposition. On the other hand, (Fig. 6B) and (Fig. 6D) images did not exhibit it. In NMTA, needle-like crystals with apatite-like morphology, approximately 0.5–1 μm in size,

were observed. In contrast, MTA-polyPS exhibited spherical apatite-like crystals ranging from approximately 0.5 to 2 μm. Although BD showed crystal formations ranging from 0.1 to 2 μm, these did not exhibit apatite-like morphology. In the case of MTA-PPL, spherical particles with an average size of approximately 1 μm were observed. ~~EDX~~ EDS Ca/P ratios of NMTA, BD, MTA-polyPS, and MTA-PPL were 1.79, 34.9, 1.70, and 3.93, respectively.

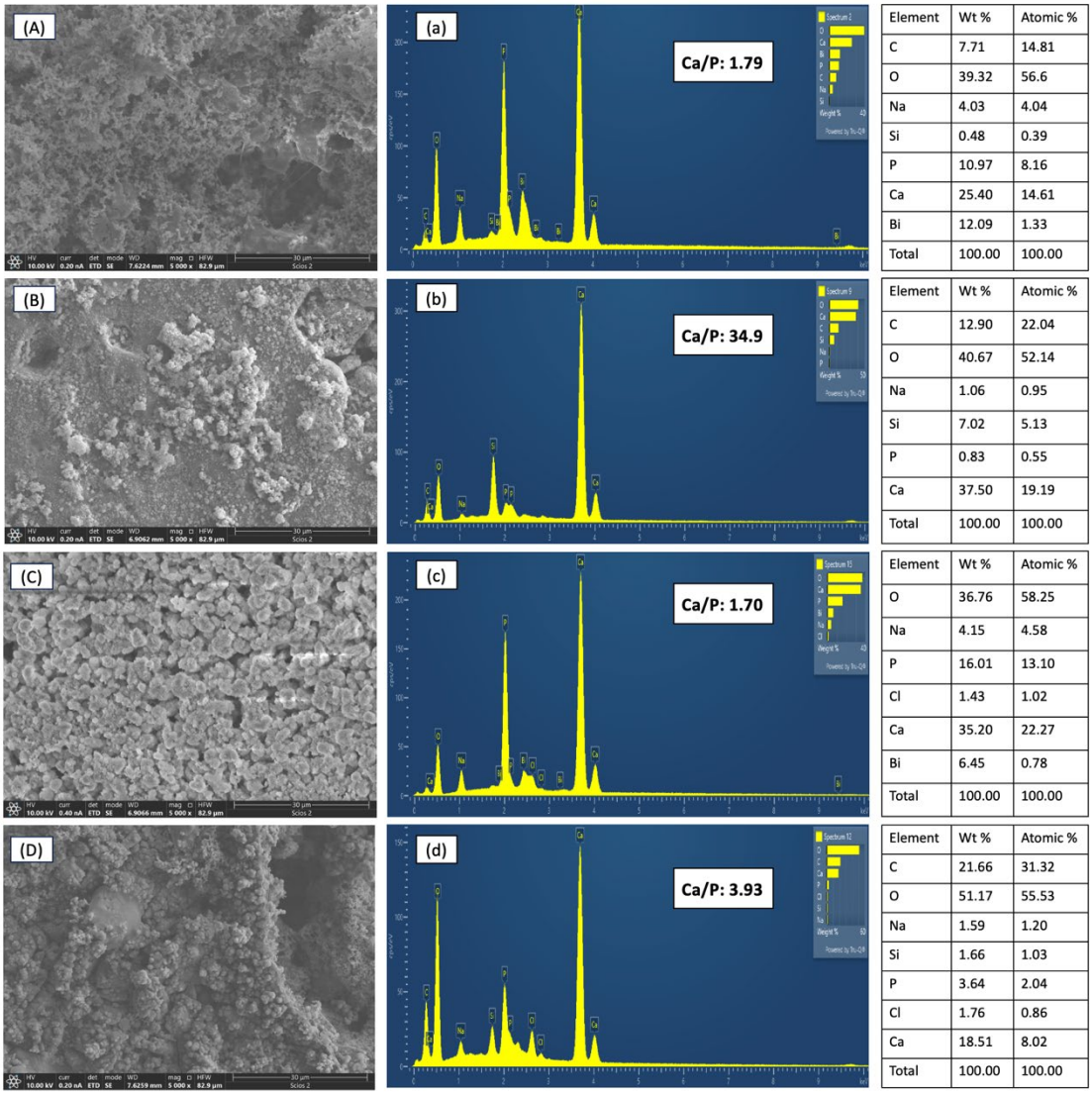

Element	Wt %	Atomic %
C	7.71	14.81
O	39.32	56.6
Na	4.03	4.04
Si	0.48	0.39
P	10.97	8.16
Ca	25.40	14.61
Bi	12.09	1.33
Total	100.00	100.00

Element	Wt %	Atomic %
C	12.90	22.04
O	40.67	52.14
Na	1.06	0.95
Si	7.02	5.13
P	0.83	0.55
Ca	37.50	19.19
Total	100.00	100.00

Element	Wt %	Atomic %
O	36.76	58.25
Na	4.15	4.58
P	16.01	13.10
Cl	1.43	1.02
Ca	35.20	22.27
Bi	6.45	0.78
Total	100.00	100.00

Element	Wt %	Atomic %
C	21.66	31.32
O	51.17	55.53
Na	1.59	1.20
Si	1.66	1.03
P	3.64	2.04
Cl	1.76	0.86
Ca	18.51	8.02
Total	100.00	100.00

Fig. 5: The results of SEM for each specimen of low magnification (×5000) where (A) NMTA, (B) BD (C) MTA-polyPS, (D) MTA-PPL), and EDS analysis with Ca/P ratio: (a) for (A), (b) for (B), (c) for (C), and (d) for (D).

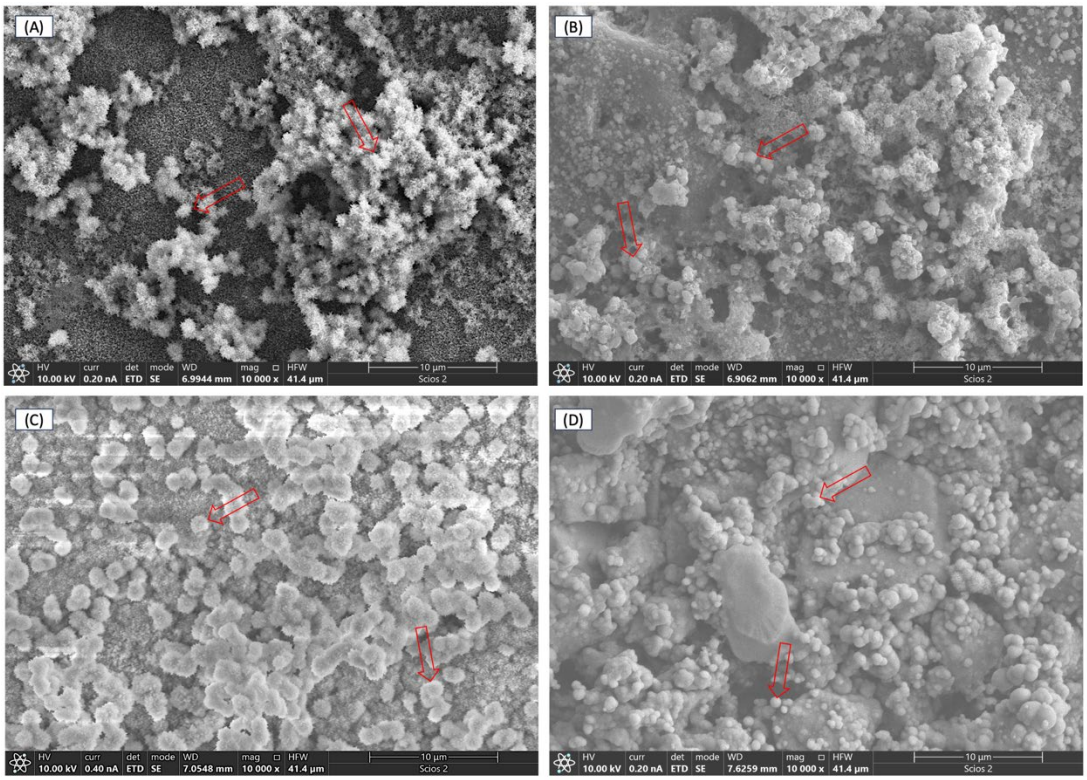

Fig. 6: The results of scanning electron microscopy for each specimen at high magnification (×10000; (A) NMTA, (B) BD (C) MTA-polyPS, (D) MTA-PPL) showing mineral deposition or particles (red arrow).

3.5 Fourier Transform Infrared Analysis

The results of FTIR analysis of each specimen, time 0 (baseline) and 28 days in PBS immersion, are presented in Fig. 7. At time 0 (baseline), only MTA-polyPS exhibited PO stretching of hydroxyapatite peaks at wavenumbers 560.89 cm^{-1}, 599.60 cm^{-1}, and 1038.23 cm^{-1} in both sections [A] and [B]. On the other hand, NMTA exhibited PO stretching of hydroxyapatite peaks at 556.3 cm^{-1} and 1053.9 cm^{-1}, and MTA-polyPS exhibited peaks at 583.1 cm^{-1}, 599.60 cm^{-1}, and 1038.23 cm^{-1} in both sections [A] and [B] in 28 days. The stronger peaks of MTA-polyPS in 28 days were confirmed than time 0. The peaks of NMTA were observed relatively weaker in 28 days.

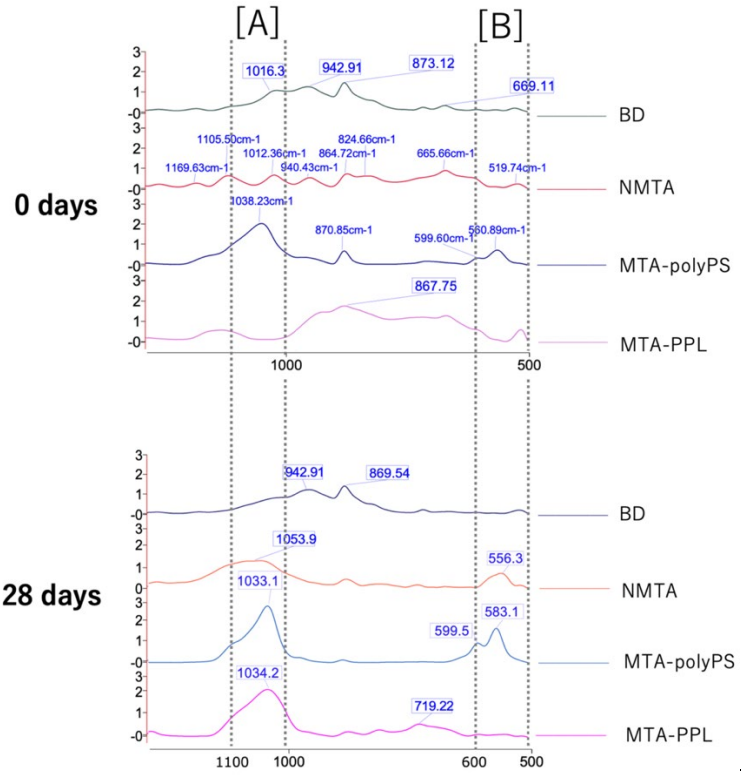

Fig. 7: The results of FTIR analysis of each specimen, time 0, and time aging. The spectra from top to bottom of the figure are BD, NMTA, MTA-polyPS, and MTA-PPL, respectively. In the wavelength range between 1000 cm^{-1} to 1100 cm^{-1} in section [A], and the spectra range between 500 cm^{-1} to 600 cm^{-1} in section [B], it is possible to observe the most representative peaks of apatite deposition.

4. DISCUSSION

The hypothesis that the incorporation of polyPS or PPL in an MTA cement would enhance its physicochemical and apatite precipitation behavior was rejected. Although the incorporation of PPL did not result in notable improvements, the significant enhancement observed with polyPS was sufficient to reject the null hypothesis regarding the overall effect of these additives on the cement's performance. The reason for such a conclusion is related to the results obtained in the different laboratory tests performed in this study.

Based on the solubility test results, MTA-PPL demonstrated the highest solubility among all groups, with statistically

significant differences ($P < 0.05$). This may be attributed to the inherent water solubility of pullulan, which possesses hydrophilic phosphate groups. It therefore may have absorbed excessive water, causing an alteration of the setting reaction as well as great porosity [37]. BD exhibited higher solubility than NMTA; this result is in accordance with a previous study that showed higher solubility in BD than conventional MTA, such as ProRoot™ MTA [38]. Since NMTA is also based on Portland cement and exhibits a composition similar to that of ProRoot™ MTA, it is assumed to have comparable chemical characteristics [10]. The higher solubility of BD may be attributed to its water-soluble additives such as $CaCl_2$, and less dense matrix compared to ProRoot™ MTA [39]. Considering the requirements of the ISO 6876:2012 standard [40], which specifies that a set sealer should be less soluble than 3% in distilled water, BD and MTA-PPL, which have comparatively higher solubility, may not be suitable for use as sealers [41][42]. As no significant difference in solubility was found between NMTA and MTA-polyPS ($P > 0.05$), and both exhibited relatively low values, they may be more suitable as sealers compared to BD and MTA-PPL.

Alkaline pH is important in biocompatibility, antibacterial activity, and osteogenic potential [43]. NMTA exhibited the highest pH at all time points, followed by BD. Previous studies have also reported that the pH of BD tends to be slightly lower than that of conventional MTA, consistent with the findings of the present study [44][45]. The pH values observed for NMTA and BD in this study were in close agreement with the results of previous studies involving ProRoot™ MTA and BD [32][46]. MTA-polyPS and MTA-PPL, which were based on NMTA incorporated with phosphate groups, exhibited significantly lower pH than NMTA at 3 h and 24 h ($P < 0.05$), but the pH of MTA-PPL was not significantly different from that of NMTA at 7 and 24 days ($P > 0.05$), whereas MTA-polyPS exhibited significantly lower pH values than NMTA at all measurement time points ($P < 0.05$). However, at 28 days, the pH of MTA-polyPS was no longer significantly different

from that of BD and MTA-PPL ($P > 0.05$). Therefore, it can be affirmed that the effect of the polyPS and PPL on the pH of NMTA is only limited in the initial stage, and this difference is unlikely to have a significant clinical impact.

BD exhibited the highest cumulative Ca^{2+}-releasing activity, with statistically significant differences ($P < 0.05$). This result is consistent with previous studies reporting that BD releases significantly more Ca^{2+} than conventional MTA [46][47]. Although both are CSC doped with phosphate compounds, MTA-PPL showed significantly higher Ca^{2+} release than NMTA at 28 days ($P < 0.05$), while MTA-polyPS exhibited the lowest release throughout all periods, with significantly lower values than NMTA after 24 h ($P < 0.05$). This result may suggest that either the higher solubility of MTA-PPL or the greater PO_4^{3-} release in MTA-polyPS led to apatite-like precipitation, thereby lowering the cumulative Ca^{2+}concentration in the solution.

BD showed the significantly shortest setting time; the the absence of Bi_2O_3 and in particular the presence of $CaCl_2$ and other accelerators contained in the liquid may have acted as an accelerator and regulated the setting reaction [13][48]. MTA-polyPS exhibited significantly shorter initial and final setting time than NMTA ($P < 0.05$). This was probably due to polyPS influencing the tricalcium silicate's and dicalcium silicate's hydration reaction, enhancing the precipitation of insoluble calcium-silicate hydrate and $Ca(OH)_2$ crystals [49]. The significantly lower pH and cumulative Ca^{2+}-releasing activity of MTA-polyPS compared to NMTA throughout all periods suggest that polyPS may consume $Ca(OH)_2$ during the calcium silicate hydration reaction, as the reduced formation of $Ca(OH)_2$ likely contributes to both the lower pH and diminished Ca^{2+} release [50]. This can be attributed to the strong affinity of poly-P for metal ions, particularly Ca^{2+}, and their ability to chelate Ca^{2+}, leading to the formation of insoluble precipitates and consequently reducing calcium availability [51]. PO_4^{3-} from poly-PS might react with the calcium hydroxide to form amorphous phosphate, which

eventually yields apatite-like precipitation [52]. Furthermore, MTA-PPL also exhibited significantly shorter initial and final setting time with a significant lower pH than NMTA at 3 h and 24 h ($P < 0.05$), but there were no significant differences ($P > 0.05$) in Ca^{2+} release between NMTA and MTA-PPL at 3 h and 24 h. The incorporation of natural modifier polymers such as fucoidan into MTA was reported to improve the setting time as a result of the acceleration of the hydration process by its cross-linking structure [53]. Therefore, the shorter setting time of MTA-PPL compared to NMTA may be primarily attributed to its polymeric structure, with the influence of PO_4^{3-} release considered negligible. Furthermore, the experimental results showing that MTA-polyPS exhibited lower pH and Ca^{2+} release than NMTA, whereas MTA-PPL demonstrated values comparable to NMTA, further support the hypothesis that MTA-polyPS contains a higher concentration of PO_4^{3-} than MTA-PPL.

Concerning the bioactivity of apatite precipitation behavior, SEM/EDS analysis showed that EDS Ca/P ratio of NMTA and MTA-polyPS were 1.79 and 1.70, respectively (Fig.5). Considering that the EDS Ca/P ratio of HAp-like precipitation is within the range of around 1.5 to 1.8 [54][55], it can be said that NMTA and MTA-polyPS have the potential to form HAp-like precipitation. This result coincides with the apatite-like precipitation of NMTA and MTA-polyPS observed in high-magnification SEM surface images (Fig. 6). Notably, the EDS Ca/P ratio of 1.70 observed in MTA-polyPS is close to the theoretical stoichiometric value of HAp, indicating that MTA-polyPS may have formed crystals more similar to ideal HAp than those formed by NMTA.

Furthermore, FTIR analysis also supported this result. In the FTIR analysis of NMTA and MTA-polyPS after aging in PBS immersion, PO stretching of HAp peaks at 500 cm^{-1} to 600 cm^{-1} and 1000 cm^{-1} to 1100 cm^{-1} were confirmed (Fig.7) [11]. MTA-polyPS might be a more promising HAp-forming material because the HAp peaks of MTA-polyPS were confirmed

more clearly than those of NMTA. At baseline, only MTA-polyPS exhibited HAp peaks in both sections [A] and [B]. This could mean MTA-polyPS has the potential to form HAp at an early stage compared with NMTA. These results support the idea that conventional MTAhas the potential to form HAp when immersed in PBS [11][56]. On the other hand, in this limited study, BD and MTA-PPL did not form apatite-like precipitation. Some other studies have shown that BD possesses the potential to induce the crystallization of minerals composed of calcium and phosphates subsequent prolonged PBS immersion [57][58]. However, it could be said that such a crystallization is only a kind of amorphous calcium-phosphate, not HAp. The reason MTA-PPL did not form apatite-like precipitation is uncertain; however, considering MTA-PPL was based on NMTA, it might be said that PPL interfered with the apatite precipitation when incorporated in NMTA. Otherwise, the absence of apatite precipitation in BD and MTA-PPL may also be attributed to their higher solubility than NMTA and MTA-polyPS, which could impair the material's ability to induce apatite precipitation and maintain surface stability.

Several studies have shown that MTA-PPL displays positive bioactivities, such as promoting excellent healing responses in the pulp tissue and facilitating complete mineral tissue formation, making it effective as a direct pulp capping material [9][20][21]. MTA-PPL showed comparable calcium ion-releasing activity and significantly shorter setting time compared with NMTA, but the higher solubility of MTA-PPL should be considered to apply it in the clinic, especially as a sealer, because the stability of the material may be the most critical factor from a long-term perspective [41][42]. On the other hand, MTA-polyPS showed significantly shorter setting time than MTA-PPL, comparable solubility with NMTA, and excellent apatite precipitation behavior. This behavior is essential for increasing the sealing ability between the material and the dentin wall; such a characteristic may also influence the regeneration and remineralization of teeth [59]. In comparison to the initial setting time of NMTA (93 min), the markedly reduced times observed for MTA-PPL (46.6 min,

approximately half) and MTA-polyPS (16.4 min, approximately one-fifth) are presumed to significantly enhance handling characteristics and clinical applicability [60][61]. Nevertheless, a more comprehensive assessment, including flowability and film thickness measurements, is warranted to substantiate these improvements.

The release of Ca^{2+} from dental materials has traditionally been regarded as a critical factor in the formation of HAp [62][63]. It is noteworthy that the current study suggested that Ca^{2+} release was not essential for HAp formation and apatite precipitation behavior. The Ca^{2+} release activity of MTA-polyPS was significantly lower compared to the other experimental groups ($P < 0.05$). While BD exhibited significantly higher Ca^{2+} release to the other experimental groups ($P < 0.05$), it resulted in almost no apatite precipitation behavior. In this context, the significantly lower Ca^{2+} release observed in MTA-polyPS may be attributed to the immediate utilization of the released Ca^{2+} for apatite precipitation, which may have limited the increase in Ca^{2+} concentration in the surrounding solution. This is consistent with the notion that the release of Ca^{2+} from the material surface, followed by the subsequent formation of an apatite layer, plays a key role in enhancing the bioactivity of CSCs through HAp formation[64][65]. Furthermore, apatite nucleation requires a localized supersaturation of Ca^{2+} and PO_4^{3-}. In PBS, where PO_4^{3-} are uniformly distributed, such conditions may not be achieved. In contrast, PO_4^{3-} released directly from the material surface can locally interact with Ca^{2+}, promoting heterogeneous nucleation and subsequent apatite precipitation [66].

Some studies have concluded that lower Ca^{2+} release in CSCs correlates with reduced HAp formation [67][68]; however, Ca^{2+}release may be primarily associated with dentin formation or the activation of dental pulp stem cells involved in the formation of reparative dentin matrix [69][70]. Additionally, given that apatite-like crystalline deposits from CSC were observed with relatively lower Ca/P ratios in PBS immersion, it suggests that PO_4^{3-} may play a crucial role in HAp

formation [71]. Previous studies have already shown that PO_4^{3-} is essential to form HAp in human bone [72][73]. Therefore, it can be suggested that PO_4^{3-} may be a more critical factor in the formation of HAp and apatite precipitation than Ca^{2+} in endodontic procedures. Future *in vivo* studies on MTA-polyPS are anticipated to shed further light on this.

The limitations of this study lie in the fact that, although it provides valuable insights into the physicochemical properties and apatite precipitation of experimental calcium silicate-based cements containing short-chain inorganic polyphosphate, further research is required to fully elucidate their clinical applicability and bioactivity. It has been reported that incorporating phosphorylated pullulan into calcium silicate-based cements can improve its handling properties and adhesion to tooth structure; however, further evaluation is needed to determine whether similar effects can be achieved by incorporating short-chain inorganic polyphosphate. In addition, further studies should be conducted to evaluate the bioactivity in forming hydroxyapatite of experimental materials under more clinical conditions, such as immersion in simulated body fluid, and to investigate how MTA-polyPS is involved in the formation of hydroxyapatite using methods such as X-ray diffraction, nuclear magnetic resonance spectroscopy, gene expression, protein, and functional analysis.

5. CONCLUSIONS

Doping MTAs with additives containing phosphate groups, such as short-chain inorganic polyphosphate, may reduce the setting time and enhance apatite precipitation behavior without significantly affecting pH or solubility. Indeed, phosphate ions play a more critical role than calcium ions in the formation of hydroxyapatite and apatite precipitation.

Acknowledgement

This work was supported by JST SPRING, Grant Number JPMJSP2119. Kenta Tsuchiya reports article publishing charges was provided by Japan Science and Technology Agency (JST). If there are other authors, they declare that they have no known competing financial interests or personal relationships that could have appeared to influence the work reported in this paper.

REFERENCES

[1] Fuss Z, Trope M. Root perforations: classification and treatment choices based on prognostic factors. Endod Dent Traumatol 1996;12:255–64.

[2] Okiji T, Yoshiba K. Reparative Dentinogenesis Induced by Mineral Trioxide Aggregate: A Review from the Biological and Physicochemical Points of View. Int J Dent 2009;2009:1–12. https://doi.org/10.1155/2009/464280.

[3] Saghiri MA, Orangi J, Asatourian A, Gutmann JL, Garcia-Godoy F, Lotfi M, et al. Calcium silicate-based cements and functional impacts of various constituents. Dent Mater J 2017;36:8–18. https://doi.org/10.4012/dmj.2015-425.

[4] Aeinehchi M, Eslami B, Ghanbariha M, Saffar AS. Mineral trioxide aggregate (MTA) and calcium hydroxide as pulp-capping agents in human teeth: a preliminary report. Int Endod J 2002;36:225–31.

[5] Matsuura T, Ziauddin SM, Kawata-Matsuura VKS, Sugimoto K, Yamada S, Yoshimura A. Long-term clinical and radiographic evaluation of the effectiveness of direct pulp capping materials: A meta-analysis. Dent Mater J 2021;40:1–7. https://doi.org/10.4012/dmj.2020-043.

[6] Palczewska-Komsa M, Kaczor-Wiankowska K, Nowicka A. New bioactive calcium silicate cement mineral trioxide aggregate repair high plasticity (Mta hp)— a systematic review. Materials 2021;14. https://doi.org/10.3390/ma14164573.

[7] Araghi S. Effect of temperature on the setting time of Mineral Trioxide Aggregate (MTA). J Med Life 2015;8:88–91.

[8] Ber BS, Hatton JF, Stewart GP. Chemical Modification of ProRoot MTA to Improve Handling Characteristics and Decrease Setting Time. J Endod 2007;33:1231–4. https://doi.org/10.1016/j.joen.2007.06.012.

[9] Pedano MS, Li X, Camargo B, Hauben E, De Vleeschauwer S, Yoshihara K, et al. Injectable phosphopullulan-functionalized calcium-silicate cement for pulp-tissue engineering: An in-vivo and ex-vivo study. Dental Materials 2020;36:512–26. https://doi.org/10.1016/j.dental.2020.01.011.

[10] Tsuchiya K, Sauro S, Sano H, Matinlinna JP, Yamauti M, Hoshika S, et al. Clinical applications and classification of calcium silicate-based cements based on their history and evolution: a narrative review. Clin Oral Investig 2025;29. https://doi.org/10.1007/s00784-025-06274-9.

[11] Maciel Pires P, Ionescu AC, Pérez-Gracia MT, Vezzoli E, Soares IPM, Brambilla E, et al. Assessment of the remineralisation induced by contemporary ion-releasing materials in mineral-depleted dentine. Clin Oral Investig

2022;26:6195–207. https://doi.org/10.1007/s00784-022-04569-9.

[12] Malkondu Ö, Kazandağ MK, Kazazoğlu E. A review on biodentine, a contemporary dentine replacement and repair material. Biomed Res Int 2014;2014. https://doi.org/10.1155/2014/160951.

[13] Kaur M, Singh H, Dhillon JS, Batra M, Saini M. MTA versus biodentine: Review of literature with a comparative analysis. Journal of Clinical and Diagnostic Research 2017;11:ZG01–5. https://doi.org/10.7860/JCDR/2017/25840.10374.

[14] Możyńska J, Metlerski M, Lipski M, Nowicka A. Tooth Discoloration Induced by Different Calcium Silicate–based Cements: A Systematic Review of In Vitro Studies. J Endod 2017;43:1593–601. https://doi.org/10.1016/j.joen.2017.04.002.

[15] Pedano MS, Li X, Yoshihara K, Van Landuyt K, Van Meerbeek B. Cytotoxicity and bioactivity of dental pulp-capping agents towards human tooth-pulp cells: A systematic review of in-vitro studies and meta-analysis of randomized and controlled clinical trials. Materials 2020;13. https://doi.org/10.3390/ma13122670.

[16] Enevoldsen BS, Schmidt F. The formation of alpha-1, 4:alpha-1, 6-linked oligosaccharides derived from pullulan. Biochem Soc Trans 1975;3:87–9.

[17] Kimotot T, Shibuya T, Shiobara S. Safety Studies of a Novel Starch, Pullulan: Chronic Toxicity in Rats and Bacterial Mutagenicity*. Food and Chemical Toxicology 1997;35:323–9.

[18] Shingel KI. Current knowledge on biosynthesis, biological activity, and chemical modification of the exopolysaccharide, pullulan. Carbohydr Res 2004;339:447–60. https://doi.org/10.1016/j.carres.2003.10.034.

[19] Takahata T, Okihara T, Yoshida Y, Yoshihara K, Shiozaki Y, Yoshida A. Bone engineering by phosphorylated-pullulan and beta-TCP composite. Biomed Mater 2015;10.

[20] Toida Y, Kawano S, Islam R, Jiale F, Chowdhury AFMA, Hoshika S, et al. Pulpal response to mineral trioxide aggregate containing phosphorylated pullulan-based capping material. Dent Mater J 2022;41:126–33. https://doi.org/10.4012/dmj.2021-153.

[21] Islam R, Toida Y, Chen F, Tanaka T, Inoue S, Kitamura T, et al. Histological evaluation of a novel phosphorylated pullulan-based pulp capping material: An in vivo study on rat molars. Int Endod J 2021;54:1902–14. https://doi.org/10.1111/iej.13587.

[22] Lonetti A, Szijgyarto Z, Bosch D, Loss O, Azevedo C, Saiardi A. Identification of an evolutionarily conserved family of inorganic polyphosphate endopolyphosphatases. Journal of Biological Chemistry 2011;286:31966–74. https://doi.org/10.1074/jbc.M111.266320.

[23] Leyhausen G, Lorenz B, Zhu H, Geurtsen W, Bohnensack R, Müller WEG, et al. Inorganic polyphosphate in human osteoblast-like cells. Journal of Bone and Mineral Research 1998;13:803–12. https://doi.org/10.1359/jbmr.1998.13.5.803.

[24] Orriss IR, Key ML, Brandao-Burch A, Patel JJ, Burnstock G, Arnett TR. The regulation of osteoblast function and bone mineralisation by extracellular nucleotides: The role of P2X receptors. Bone 2012;51:389–400. https://doi.org/10.1016/j.bone.2012.06.013.

[25] Shiba T, Nishimura D, Kawazoe Y, Onodera Y, Tsutsumi K, Nakamura R, et al. Modulation of mitogenic activity of fibroblast growth factors by inorganic polyphosphate. Journal of Biological Chemistry 2003;278:26788–92. https://doi.org/10.1074/jbc.M303468200.

[26] Shiba T. Inorganic polyphosphate and its chain length dependency in tissue regeneration including bone remodeling and teeth whitening. Inorganic Polyphosphates in Eukaryotic Cell 2016:139–58. https://doi.org/10.1073/pnas.262655199.

[27] Tanaka T, Terashima M, Iketani Y, Kawazoe Y, Shiba T, Manabe A. Suppression of Demineralization by inorganic Polyphosphates with Optimum Chain Length for Stain Removal and Prevention of Stain Deposition. The Japanese Journal of Conservative Dentistry 2021;64:107–15.

[28] Kato K, Morita K, Hirata I, Doi K, Kubo T, Kato K, et al. Enhancement of calcification by osteoblasts cultured on hydroxyapatite surfaces with adsorbed inorganic polyphosphate. In Vitro Cell Dev Biol Anim 2018;54:449–57. https://doi.org/10.1007/s11626-018-0257-3.

[29] Jacy RCJ, Lourenco CS, Americo BC, Mario ACS, Simonides C, Manel DSN. Solubility and Dimensional Change after Setting of Root Canal Sealers: A Proposal for Smaller Dimensions of Test Samples. J Endod 2007;33:1110–6.

[30] Tedesco M, Vitali FC, Bortoluzzi EA, Garcia L da FR, Teixeira C da S. Analysis of physicochemical properties of endodontic sealers containing rhodamine B. J Mech Behav Biomed Mater 2023;140. https://doi.org/10.1016/j.jmbbm.2023.105699.

[31] Ghazvini SA, Abdo Tabrizi M, Kobarfard F, Baghban AA, Asgary S. Ion release and pH of a new endodontic cement, MTA and Portland cement. Iran Endod J 2009;4:74–82.

[32] Galal M, Zaki DY, Rabie MI, El-Shereif SM, Hamdy TM. Solubility, pH change, and calcium ion release of low solubility endodontic mineral trioxide aggregate. Bull Natl Res Cent 2020;44. https://doi.org/10.1186/s42269-020-00303-1.

[33] ANSI/ADA Specification N57, Endodontic Sealing Materials. Chicago, IL : ANSI/ADA, 2000. n.d.

[34] Guo YJ, Du TF, Li HB, Shen Y, Mobuchon C, Hieawy A, et al. Physical properties and hydration behavior of a fast-setting bioceramic endodontic material. BMC Oral Health 2016;16. https://doi.org/10.1186/s12903-016-0184-1.

[35] Öztürk Z, Bal C, Güngörmüş M, Aksoy M. Effects of a mineralization-promoting peptide on the physical and chemical properties of mineral trioxide aggregate. J Mech Behav Biomed Mater 2023;138. https://doi.org/10.1016/j.jmbbm.2022.105570.

[36] Alambiaga-Caravaca AM, Chou YF, Moreno D, Aparicio C, López-Castellano A, Feitosa VP, et al. Characterisation of experimental flowable composites containing fluoride-doped calcium phosphates as promising remineralising materials: “Smart” composites doped with fluoride-doped calcium phosphate. J Dent 2024;143. https://doi.org/10.1016/j.jdent.2024.104906.

[37] Oğuzhan P, Yangılar F. Pullulan: Production and usage in food ındustry. African Journal of Food Science and Technology 2013;4:57–63.

[38] Kaup M, Schäfer E, Dammaschke T. An in vitro study of different material properties of Biodentine compared to ProRoot MTA. Head Face Med 2015;11. https://doi.org/10.1186/s13005-015-0074-9.

[39] Camilleri J. Investigation of Biodentine as dentine replacement material. J Dent 2013;41:600–10. https://doi.org/10.1016/j.jdent.2013.05.003.

[40] Dentistry-Root canal sealing materials INTERNATIONAL STANDARD ISO 6876. 2012.

[41] Espir CG, Guerreiro-Tanomaru JM, Spin-Neto R, Chávezandrade GM, Berbert FLCV, Tanomaru-Filho M. Solubility and bacterial sealing ability of MTA and root-end filling materials. Journal of Applied Oral Science 2016;24:121–5. https://doi.org/10.1590/1678-775720150437.

[42] Fristad I, Haug S, Bårdsen A. Biological properties versus solubility of endodontic sealers and cements. Biomater Investig Dent 2024;11:54–65. https://doi.org/10.2340/biid.v11.40863.

[43] Poggio C, Dagna A, Ceci M, Meravini MV, Colombo M, Pietrocola G. Solubility and pH of bioceramic root canal sealers: A comparative study. J Clin Exp Dent 2017;9:e1189–94. https://doi.org/10.4317/jced.54040.

[44] Pelepenko LE, Saavedra F, Antunes TBM, Bombarda GF, Gomes BPFA, Zaia AA, et al. Physicochemical, antimicrobial, and biological properties of White-MTAFlow. Clin Oral Investig 21AD:663–72. https://doi.org/10.1007/s00784-020-03543-7/Published.

[45] Soundarya N, Manoharan M, Veerabadhran MM, Gawthaman M, Vinodh S, Kamatchi M. Comparative Evaluation of pH, Calcium Ion Release, and Setting Time of Premixed and Freshly Mixed Tricalcium Silicate-based Endodontic Materials: An In Vitro Study. Int J Clin Pediatr Dent 2024;17:1330–4. https://doi.org/10.5005/jp-journals-10005-3015.

[46] Khalil Yousef M, Abuzeid S, Taha Hassan Abu Zeid S, Alothmani OS, Khalil Yousef Biodentine M. Biodentine and Mineral Trioxide Aggregate: An Analysis of Solubility, pH Changes and Leaching Elements. Life Sci J 2015;12:1097–8135.

[47] Herrera-Trinidad R, Molinero-Mourelle P, Fonseca M, Weber AR, Vera V, Mena ML, et al. Assessment of pH Value and Release of Calcium Ions in Calcium Silicate Cements: An In Vitro Comparative Study. Materials 2023;16. https://doi.org/10.3390/ma16186213.

[48] Kadali NS, Alla RK, AV R, MC SS, Raju Mantena S, Raju RV. An overview of composition, properties, and applications of Biodentine. International Journal of Dental Materials 2021;03:120–6. https://doi.org/10.37983/ijdm.2021.3404.

[49] Camilleri J. Hydration mechanisms of mineral trioxide aggregate. Int Endod J 2007;40:462–70. https://doi.org/10.1111/j.1365-2591.2007.01248.x.

[50] Chang S-W. Chemical characteristics of mineral trioxide aggregate and its hydration reaction. Restor Dent Endod 2012;37:188. https://doi.org/10.5395/rde.2012.37.4.188.

[51] Mingyue Song, Leping Dang, Hongyuan Wei. Evaluation of calcium binding capacity of chelating agents in calcium carbonate suspension and effects on calcium distribution of calcium chelating agents. Aust J Chem 2021;74:557–63.

[52] Tay FR, Pashley DH, Rueggeberg FA, Loushine RJ, Weller RN. Calcium phosphate phase transformation produced by the interaction of the portland cement component of white mineral trioxide aggregate with a phosphate-containing fluid. J Endod 2007;33:1347–51.

[53] Kim M, Hayashi M, Yu B, Lee TK, Kim RH, Jo DW. Effects of Fucoidan Powder Combined with Mineral Trioxide Aggregate as a Direct Pulp-Capping Material. Polymers (Basel) 2022;14. https://doi.org/10.3390/polym14122315.

[54] Tariq U, Haider Z, Chaudhary K, Hussain R, Ali J. Calcium to phosphate ratio measurements in calcium phosphates using LIBS. J Phys Conf Ser, vol. 1027, Institute of Physics Publishing; 2018. https://doi.org/10.1088/1742-6596/1027/1/012015.

[55] Alambiaga-Caravaca AM, Chou YF, Moreno D, Aparicio C, López-Castellano A, Feitosa VP, et al. Characterisation of experimental flowable composites containing fluoride-doped calcium phosphates as promising remineralising materials: “Smart” composites doped with fluoride-doped calcium phosphate. J Dent 2024;143. https://doi.org/10.1016/j.jdent.2024.104906.

[56] Sarkar NK, Caicedo R, Ritwik P, Moiseyeva R, Kawashima I. Physicochemical basis of the biologic properties of mineral trioxide aggregate. J Endod 2005;31:97–100. https://doi.org/10.1097/01.DON.0000133155.04468.41.

[57] Han L, Okiji T. Uptake of calcium and silicon released from calcium silicate-based endodontic materials into root canal dentine. Int Endod J 2011;44:1081–7. https://doi.org/10.1111/j.1365-2591.2011.01924.x.

[58] Kim JR, Nosrat A, Fouad AF. Interfacial characteristics of Biodentine and MTA with dentine in simulated body fluid. J Dent 2015;43:241–7. https://doi.org/10.1016/j.jdent.2014.11.004.

[59] Parirokh M, Torabinejad M. Mineral Trioxide Aggregate: A Comprehensive Literature Review-Part III: Clinical Applications, Drawbacks, and Mechanism of Action. J Endod 2010;36:400–13. https://doi.org/10.1016/j.joen.2009.09.009.

[60] Tilakchand M, Pandey P, Shetty P, Naik B, Shetti S, Nirmala C. The comparative evaluation of various additives on setting time and compressive strength of MTA Plus: An in vitro study. Endodontology 2021;33:36–42. https://doi.org/10.4103/endo.endo_75_20.

[61] Pushpalatha C, Dhareshwar V, Sowmya S V., Augustine D, Vinothkumar TS, Renugalakshmi A, et al. Modified Mineral Trioxide Aggregate—A Versatile Dental Material: An Insight on Applications and Newer Advancements. Front Bioeng Biotechnol 2022;10. https://doi.org/10.3389/fbioe.2022.941826.

[62] Belal RSI, Edanami N, Yoshiba K, Yoshiba N, Ohkura N, Takenaka S, et al. Comparison of calcium and hydroxyl ion release ability and in vivo apatite-forming ability of three bioceramic-containing root canal sealers. Clin Oral Investig 2022;26:1443–51. https://doi.org/10.1007/s00784-021-04118-w.

[63] Tuygunov N, Khairunnisa Z, Yahya NA, Abdul Aziz A, Zakaria MN, Israilova NA, et al. Bioactivity and remineralization potential of modified glass ionomer cement: A systematic review of the impact of calcium and phosphate ion release. Dent Mater J 2024;43:1–10. https://doi.org/10.4012/dmj.2023-132.

[64] Gandolfi MG, Taddei P, Tinti A, De Dorigo ES, Rossi PL, Prati C. Kinetics of apatite formation on a calcium-silicate cement for root-end filling during ageing in physiological-like phosphate solutions. Clin Oral Investig 2010;14:659–68. https://doi.org/10.1007/s00784-009-0356-3.

[65] Camilleri J, Sorrentino F, Damidot D. Investigation of the hydration and bioactivity of radiopacified tricalcium silicate cement, Biodentine and MTA Angelus. Dental Materials 2013;29:580–93. https://doi.org/10.1016/j.dental.2013.03.007.

[66] Habraken WJEM, Tao J, Brylka LJ, Friedrich H, Bertinetti L, Schenk AS, et al. Ion-association complexes unite classical and non-classical theories for the biomimetic nucleation of calcium phosphate. Nat Commun 2013;4. https://doi.org/10.1038/ncomms2490.

[67] Arandi NZ, Thabet M. Minimal Intervention in Dentistry: A Literature Review on Biodentine as a Bioactive Pulp Capping Material. Biomed Res Int 2021;2021. https://doi.org/10.1155/2021/5569313.

[68] Yamamoto S, Han L, Noiri Y, Okiji T. Evaluation of the Ca ion release, pH and surface apatite formation of a prototype tricalcium silicate cement. Int Endod J 2017;50:e73–82. https://doi.org/10.1111/iej.12737.

[69] Song M, Yu B, Kim S, Hayashi M, Smith C, Sohn S, et al. Clinical and Molecular Perspectives of Reparative Dentin Formation: Lessons Learned from Pulp-Capping Materials and the Emerging Roles of Calcium. Dent Clin North Am 2017;61:93–110. https://doi.org/10.1016/j.cden.2016.08.008.

[70] Sangwan P, Sangwan A, Duhan J, Rohilla A. Tertiary dentinogenesis with calcium hydroxide: A review of proposed mechanisms. Int Endod J 2013;46:3–19. https://doi.org/10.1111/j.1365-2591.2012.02101.x.

[71] Han L, Kodama S, Okiji T. Evaluation of calcium-releasing and apatite-forming abilities of fast-setting calcium silicate-based endodontic materials. Int Endod J 2015;48:124–30. https://doi.org/10.1111/iej.12290.

[72] Michigami T, Ozono K. Roles of phosphate in skeleton. Front Endocrinol (Lausanne) 2019;10. https://doi.org/10.3389/fendo.2019.00180.

[73] Hughes EAB, Robinson TE, Bassett DB, Cox SC, Grover LM. Critical and diverse roles of phosphates in human bone formation. J Mater Chem B 2019;7:7460–70. https://doi.org/10.1039/c9tb02011j.